Regional Analysis of D2 Dopamine Receptors in Parkinson's Disease Using SPECT and Iodine-123-Iodobenzamide

Stephen E. Nadeau, Margaret W. Couch, C. Lindsay Devane and Shailendra S. Shukla

Geriatric Research, Education and Clinical Center, Department of Veterans Affairs Medical Center; Departments of Neurology and Radiology, University of Florida College of Medicine, Gainesville, FL; Department of Psychiatry, Medical University of South Carolina, Charleston, South Carolina.

The goal of this study was to examine the relationship between D2 dopamine receptor density and levodopa dosage, disease duration and dyskinesia in Parkinson's disease (PD). **Methods:** Iodine-123-iodobenzamide SPECT scans were obtained from 14 PD patients and 12 age-matched controls using a three-headed camera in conjunction with MRI and a fiducial-based image registration system to define regions of interest. Basal ganglia/cerebellum counts/voxel ratios in dorsal and ventral head of caudate and anterior and posterior putamen were measured at 30, 60, 120 and 180 min postinjection. As in ^{11}C-raclopride studies, ratios obtained at that time when they asymptomatically approach a maximum value (180 min) were accepted as the best measure of receptor density. **Results:** Among PD patients, a trend towards an inverse correlation between regional basal ganglia/cerebellum ratios and levodopa dosage achieved significance in ventral caudate (F = 6.244, p = 0.037); similarly, an inverse correlation between these ratios and disease duration achieved significance in anterior putamen (F = 13.144, p = 0.007). Ratios were significantly lower in anterior putamen in patients with dyskinesia (t = 3.068, p = 0.042). **Conclusion:** In PD, the previously observed inverse correlation between levodopa dosage and D2-receptor density appears to be most prominent in the least dopamine-depleted region, ventral caudate. There may be a genuine effect of disease duration on receptor density in putamen and reduced receptor density in anterior putamen may be associated with dyskinesia.

Key Words: dopamine receptors; D2 receptors; iodobenzamide; SPECT; Parkinson's disease

J Nucl Med 1995; 36:384–393

Satisfactory management of Parkinson's disease (PD) patients becomes progressively more difficult as the disease advances. Dyskinesias are an important contributor to late clinical decline. Several investigators have suggested that dyskinesias are related to alterations in postsynaptic dopamine receptors associated either with advancing disease or treatment of the disease (1,2). The traditional explanation has been that dyskinesias are related to receptor denervation supersensitivity, perhaps interacting with a differential pattern of dopamine depletion through the target organs of the nigrostriatal system, particularly the putamen. However, the neurophysiologic mechanism by which receptor hypersensitivity might lead to dyskinesias has not been established. Furthermore, postmortem assays of D1 and D2 dopamine receptors in the basal ganglia of PD patients have generally failed to demonstrate consistent alterations in either density or affinity, in part because of enormous patient to patient variability (3–5). The causes of this variability are uncertain but may include patient heterogeneity, inconsistent maintenance of dopaminergic medication in terminal illness and variable delay between death and receptor assay. More recently, it has become possible to assay postsynaptic dopamine receptors in vivo using PET and SPECT in conjunction with specific high-affinity receptor ligands. In vivo assay avoids some of the intrinsic limitations of postmortem studies and can be readily applied to much larger numbers and a wider variety of patients at different stages of disease. D2 dopamine receptors are the focus of the present study and have been measured with PET using ^{11}C-raclopride, and SPECT using a structurally similar benzamide with comparable affinity and specificity, $[^{123}I]$-iodobenzamide (IBZM) (6). In vivo receptor studies offer a new opportunity to detect alterations that might account for the development of dyskinesias.

This investigation incorporates two modest innovations on previous studies. The first is an improved method for quantitation of receptor density. It has become customary in both PET and SPECT studies to compute specific binding in target organs such as the basal ganglia as the difference between total binding (total counts) and nonspecific binding (e.g., counts in the cerebellum, which has been shown to have no specific binding), divided by nonspecific binding (in order to eliminate the effect of individual variability in amount of ligand entering the brain). Because this quantity, (basal ganglia−cerebellum)/cerebellum, is equal to (basal ganglia/cerebellum) − 1, the simple ratio basal ganglia/cerebellum can be used as an index of specific

binding. It has been shown that in ^{11}C-raclopride PET studies the ratio quickly rises during the minutes after intravenous injection and eventually asymptotically approaches a maximum, referred to as the transient equilibrium, which has been accepted as a good index of B_{max}, which is the total receptor density (7–9). A similar approach has been employed in SPECT D2 dopamine receptor imaging studies, but no previous clinical study has measured activity sufficiently long after injection to assure achievement of the asymptotic maximum; quite the contrary, 120 min postinjection, a time when the basal ganglia/cerebellum ratio is still rising in many patients, has been taken as the standard. Because the ratio is still rising, modest individual variability in the timing of scans can contribute considerable noise to results. In the present investigation, patients were routinely scanned four times, the last time 180 min postinjection, when basal ganglia/cerebellum ratios have stabilized.

Recently, Carson et al. (10) provided evidence that ratios of specific to nonspecific activity derived during transient equilibrium (180 min postinjection with IBZM) are greater than ratios derived at true equilibrium, defined as the peak in specific uptake (50–130 min postinjection with IBZM). Ratios derived at true equilibrium provide the optimal measure of B_{max}. However, because of the long scan times required with IBZM SPECT and the rapid change in specific uptake with time, it is impossible to precisely define the point of maximum specific uptake. Furthermore, the actual measurement of maximum specific uptake provided by IBZM SPECT will be an underestimate because it represents a 20-min integral of the rapidly varying specific uptake function. Fortunately, ratios derived during transient equilibrium are a constant linear function of ratios obtained at true equilibrium (10), and thus, provide an acceptable index of B_{max}. In addition, ratios obtained during transient equilibrium are not susceptible to the operational problems and time sensitivity associated with ratios obtained at true equilibrium because the slope of the ratio curve during transient equilibrium is constant and very close to zero.

Our second innovation was motivated by the observation that dopamine levels in PD patients are not equally depleted in all regions of the basal ganglia. Dopamine is severely depleted in the putamen, particularly posteriorly, whereas reductions in the ventral caudate are far more modest, and probably clinically insignificant in most patients (11). We hypothesized that receptor alterations potentially related to the development of dyskinesia were more likely to appear in the putamen. To test this hypothesis, we assayed receptor density on a regional basis, in dorsal (Cd_D) and ventral caudate (Cd_V), and in anterior (Put_A) and posterior putamen (Put_P).

METHODS

Subjects

Fifteen patients with PD and 14 age-matched controls (patient spouses) were recruited from the community, generally through PD support organizations. This study was approved and monitored by the Investigational Review Boards of the VA Medical Center and the University of Florida, and the Radioactive Drug Research Committee of the University of Florida. All subjects provided informed consent to participate. One control patient was excluded because of inability to tolerate an MRI scan because of claustrophobia. A second control patient and one PD patient were excluded because of technical inadequacies of the SPECT or MRI scans (fiducials missing or inadequately defined). Data on the final 14 PD patients and 12 control patients are presented in Table 1. Patients were screened by a neurologist (SEN), scored on the Unified Parkinson's Disease Rating (UPDR) (12) and Hoehn and Yahr (13) scales and administered the Mini-Mental State examination (14). All PD patients had typical disease with the triad of tremor, rigidity and bradykinesia, and all had demonstrated a clear response to dopaminergic therapy. Patients were all Hoehn and Yahr classes II or III. Dyskinesia was deemed present if observed on examination or reported in unequivocal fashion by the patient. No patients had dementia, apraxia, ataxia, autonomic dysfunction, pyramidal signs or ophthalmoplegia other than upgaze paresis. All patients were taking levodopa; many were deprenyl (see Table 1); one bromocriptine; one amantadine; four anticholinergic agents; and three were taking antidepressants. None of the controls had any evidence by history or exam of neurologic disease, and none were taking any centrally acting drugs likely to be significant. None of the patients were managed by the investigators in this study, and all were instructed to take their medication in their usual fashion. Medications were maintained to minimize disruption of the patients' lives as well as to minimize the Parkinsonian tremor, which has the potential for seriously degrading image quality. It was also important to minimize the potential alteration of dopamine receptors as a result of the 15 hr dopamine holiday that would have occurred had we withheld medications (radioligand injection was at approximately 1 p.m. in all subjects).

Materials

Iodine-123-iodobenzamide was prepared with a method adapted from Kung and Kung (15). To a sealed vial containing sodium [123]I (ca. 20 mCi in 0.1 N NaOH, no-carrier-added, specific activity 2.4 Ci/mmole × 10^5 Ci/mmole; Nordion International, Inc., Vancouver, Canada) were added (S)-(-)-2-hydroxy-6-methoxy-N-[(1-ethyl-2-pyrrolidinyl)]benzamine (BZM, 50 μg in 50 μl ethanol), and ammonium acetate pH 4.0 (0.3 ml, 0.5 M). Peracetic acid (0.48%, 100 μl, obtained by diluting commercially available 32% solution with sterile water) was added to this mixture. The reaction was allowed to proceed at room temperature for 5 min and then was quenched with sodium bisulfite (0.1 ml, 100 mg/ml). The mixture was neutralized with saturated sodium bicarbonate solution (ca. 1 ml) and the product extracted three times with ethyl acetate (3 ml × 1 ml). The combined ethyl actate layers were passed through an anhydrous sodium sulfate column (2 mm × 5 cm) and then evaporated under a jet of nitrogen. The resulting residue was dissolved in absolute ethanol (200 μl). This solution was purified by reversed phase HPLC: C_{18} column (PRP-1, 4.6 mm × 25 cm, Hamilton Co., Reno, NV); ethanol: ammonium phosphate (20 mM, pH 7.0)(80:20), 1 ml/min; QC-2000 quick count radiation detector (Bioscan Inc., Washington, DC). The fractions of eluent containing the no-carrier added product were mixed with 100 μg ascorbic acid and their volume reduced in vacuo to approximately the volume of the water present in the collected eluent (ca. 1 ml). The reduced eluant was diluted with

TABLE 1
Patient Data

Patient no.	Age (yr)	Sex	Duration PD (yr)	Daily L-DOPA	Deprenyl	H&Y	UPDR Motor	Dyskinesia	Dose injected (mCi)	Basal ganglia/cerebellum ratio (180 min)					Status
										Cd_V	Cd_D	Put_A	Put_P	Cerebellum*	
1	75	F	11	200	+	2	11	+	2.27	1.76	1.67	2.55	2.13	4.5	Excluded
2	73	F	7	750	—	2	9	—	3.47	6.71	4.30	7.51	4.08	.3	Excluded
3	72	M	5	300	—	2	18	—	6.28	1.44	1.49	1.51	0.87	6.0	Excluded
4	67	M	3	200	+	2	12	—	3.82	1.64	1.65	2.12	1.59	8.7	
5	76	M	6	400	+	2	13	—	4.83	1.91	1.70	2.16	1.67	8.8	
6	66	M	5	300	+	2	7	+	7.00	1.81	1.29	1.88	1.76	18.3	
7	75	F	16	1000	+	3	6	+	5.90	0.85	1.03	1.43	1.64	26.0	†‡
8	57	F	21	400	—	2	18	+	7.17	1.45	1.37	1.05	0.97	96.8	120 min data§
9	71	M	9	300	+	2	9	—	5.00	2.52	3.18	2.31	1.59	8.9	§
10	75	M	7	300	+	2	11	—	4.59	1.66	2.01	2.42	1.49	9.9	§
11	62	M	12	500	+	2	11	+	6.39	1.55	1.63	1.85	1.68	14.7	
12	51	F	11	150	—	3	24	—	9.00	1.99	2.00	2.14	1.81	28.6	‡§
13	68	M	14	1000	—	2	10	—	5.86	1.52	1.18	1.97	1.60	29.6	
14	85	M	9	300	—	3	17	—	3.52	2.39	1.67	2.76	1.94	2.5	Excluded
15	73	M							3.69	2.35	2.46	4.83	3.34	0.9	Excluded
16	69	F							8.15	1.90	1.87	2.00	1.69	21.8	
17	74	M							7.50	1.59	1.45	1.84	1.77	17.4	
18	70	F							4.57	1.48	1.61	2.81	2.72	1.8	Excluded
19	84	F							5.79	1.53	1.94	0.80	1.07	2.1	Excluded
20	65	F							8.20	1.82	1.36	1.93	1.83	25.3	
21	66	F							5.82	1.65	1.97	1.57	1.51	24.5	
22	76	F							7.84	2.06	1.62	2.11	1.86	18.6	
23	75	M							6.53	2.11	1.73	2.34	2.17	14.3	
24	57	M							4.21	2.09	1.76	2.30	1.98	10.7	
25	49	M							7.00	1.69	1.60	1.97	1.69	42.6	
26	67	F							9.07	1.97	1.72	1.81	1.48	28.0	

*Counts/voxel at 180 min.
†Bromocriptine and amantadine.
‡Antidepressant.
§Anticholinergic.

sufficient saline (2–10 ml) containing 100 μg ascorbic acid that a 0.5 to 1.5 mCi/ml solution of [^{123}I]BZM resulted (specific activity 2.4 Ci/mmole × 10^5 Ci/mmole). This solution was filtered through a 0.22 μm sterile filter (Millex-GS, Millipore, Marlborough, MA) into a sealed sterile vial.

The pH of the final formulation was checked to make sure that it was between 5 and 8. The integrity of the sterile filter was checked by the air bubble test. Pyrogenicity (LAL test) and sterility tests (tryptic soy broth and thioglycollate) were conducted to demonstrate that the final formulation was indeed pyrogen free and sterile.

Image Acquisition

SPECT images were acquired on a three-headed Triad 88 system (Trionix Research Laboratory, Twinsburg, OH) with ultra high-resolution collimators. The in-plane resolution of this camera is 9.3 mm FWHM. Images were acquired with each head rotating 360° in 3° steps, creating 360 raw image sets. The subject's head was positioned in the standard head holder and was instructed to remain motionless. Image acquisition required approximately 20 min. Subjects were premedicated only with oral Lugol's solution to protect the thyroid gland. Between 2.27 mCi and 9.07 mCi (84 MBq to 337 MBq) of IBZM were intravenously injected while the subject lay supine on the scanner gantry. Images were acquired between 20 and 40 min (the 30 min scan), 50 and 70 min (the 60 min scan), 110 and 130 min (the 120 min scan) and 170 and 190 min

(the 180 min scan) postinjection. T-1 weighted MRI images were obtained on a different day in axial planes on a Magnetom 1.5 Tesla scanner (Siemens, Iselin, NJ).

Markers were used to register SPECT and MRI images in the same image space (16). Prior to the experiment, semi-rigid plastic molds were fashioned from XL-100 Impression System material (JKR Laboratories, Wichita, KS) for both ears and the junction of the nose and the glabella. The distinct impression left on the molds permits reliable placement at precisely the same location on different occasions. Molds were constructed to hold Lucite discs (markers) 25 mm in diameter × 6 mm thick. For SPECT images, a small well in the center of each disc contained 50 μCi of ^{57}cobalt (Nuclear Associates, Carle Place, NY) which was clearly visible on SPECT images. For MRI scans, the well in each disc contained a 4.5 mM copper sulfate solution which was visible on MRI images.

Image Processing and Analysis

SPECT image reconstruction was performed using standard filtered backprojection with an attenuation correction factor of 0.12/cm and a 16-point cylindrical algorithm. Image smoothing was accomplished with a Hamming filter (cut-off frequency 0.9/cm). Original images were reconstructed in 64 × 64 pixel axial planes with 3.56 × 3.56 mm pixels and a 3.56 mm slice thickness. After image rotation (see below), each two successive SPECT slices were combined to yield a slice thickness of 7.12 mm (neg-

FIGURE 1. Basal ganglia ROI as defined at one level on the MRI scan.

ligibly different from the MRI slice thickness of 7.0 mm). MRI images were initially acquired in a 256 × 256 pixel format with 0.90 × 0.90 mm pixels and a 7 mm slice thickness, and transfered to the Sun workstation accompanying the Triad system. They were then converted to a 128 × 128 pixel format for faster processing (16).

Even with careful positioning of the head, the three markers rarely were contained in a single axial plane. However, the software accompanying the Triad-88 camera allowed us to rotate SPECT and MRI images until the three markers defined a single axial plane. After addition of adjacent slices to obtain a 7.12 mm slice thickness, the three markers could generally be seen on three SPECT slices. Markers generally could be seen on one or two MRI slices. Slices with maximal marker definition were chosen as the reference. This fiducial image alignment system has a demonstrated accuracy of within one acquisition pixel (3.56 mm) (16). Image slices obtained using this fiducial system are reliable at the same angle with respect to the orbitomeatal line as the slices in Appendix A.4 of the Damasio and Damasio atlas (17).

In this study we were interested exclusively in the cerebellum and the basal ganglia. The caudal second through sixth slices (the second through sixth slices from the bottom) from the A.4 Appendix of the Damasio atlas contain the portions of these structures chosen for region of interest (ROI) analysis. MRI slices corresponding to these five planes were selected together with corresponding SPECT slices from the 30, 60, 120 and 180 min scans, and analysed as a group (5 × 5 matrix of scans, each reconstructed in a 128 by 128 pixel format). Before any ROI calculations, SPECT and MRI slices were reregistered along the x and y axes such that SPECT slices were centered to the maximum extent possible over MRI slices. This correction, generally only 0.5 to 1 acquisition pixels along either axis, was done to further reduce the modest registration errors associated with complete reliance on our fiducial-based coordinate system. ROIs were defined by tracing around the border of relevant structures on the MRI slices (Fig. 1). The imaging software then allowed us to compute area and total counts in the corresponding ROI in each of the SPECT slices. Those portions of the cerebellum visible on MRI slices corresponding to the caudal second and third planes from the A.4 Appendix of the Damasio atlas were chosen (the middle 14 mm along the rostro-caudal axis of the entire cerebellum). Ventral head of caudate ROIs were taken from MRI slices corresponding to the caudal fourth and fifth planes from the A.4 Appendix. Dorsal head of caudate ROIs were taken from the MRI slice corresponding to the caudal sixth plane. Anterior and posterior putamen ROIs were taken from MRI slices corresponding to the caudal fourth and fifth planes. In occasional subjects this

routine had to be varied slightly to accommodate atypical anatomy, e.g. the head of caudate began at the caudal third (rather than fourth) slice. Values of left and right hemisphere ROIs were combined. The smallest ROIs (head of caudate) were a minimum of 201.78 × 1.78 mm pixels in area (63 mm^2). Putamen ROIs were between 190 and 310 mm^2 in area. Because head of caudate ROIs involved volume averaging with the frontal horns, we were concerned that ROI counts might be influenced by the size of the frontal horns; frontal horn size was measured but failed to correlate with head of caudate ROI counts.

Data extracted from the image analysis were loaded onto a Macintosh SE/30 computer (Apple Computer, Inc., Cupertino, CA) equipped with SPSS (Chicago, IL) and SYSTAT (Evanston, IL). Data were analyzed using regression analysis and t-tests (separate variances), with two-tailed tests of significance in all cases.
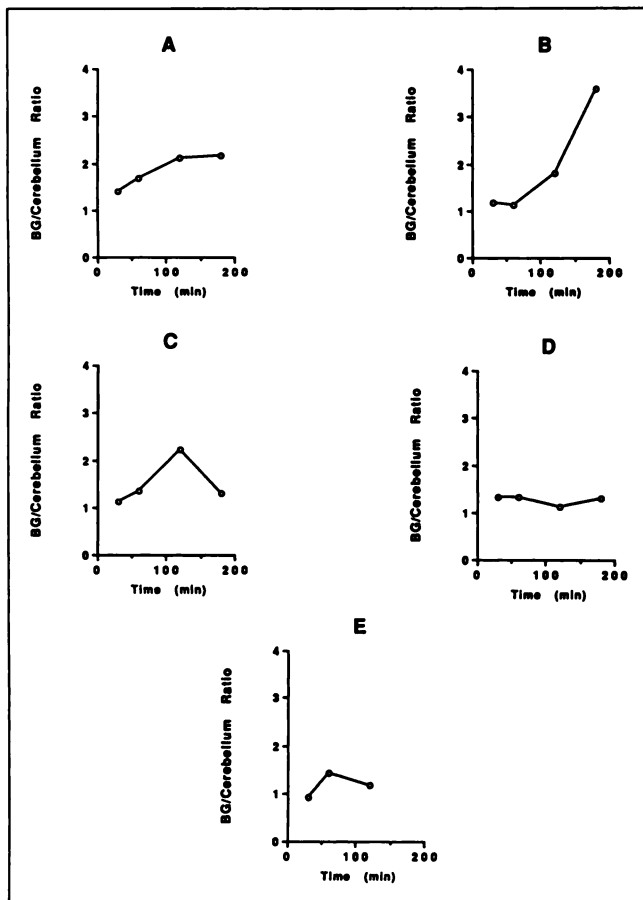
RESULTS

Pharmacokinetic Study

Basal ganglia region/cerebellum counts/voxel ratios were plotted as function of time for each subject. In general this ratio asymptotically approached a maximum between 1.5 and 2.5 at 180 min, as exemplified by the curve in Figure 2A. However, in three patients (Patients 2, 15, 18) (Fig. 2B), precisely those with the lowest cerebellar counts at 180 min, the ratio became very large at 180 min because of the very low cerebellar counts. In four patients (1, 3, 14, 19) (Fig. 2C), those with the next lowest cerebellar counts at 180 min, the ratio became unreasonably high at 120 min and declined thereafter. Because of the obvious cause for artifact in the three patients with the lowest cerebellar counts, and the evident but unexplainable artifact in the four patients with the next lowest cerebellar counts, all seven were removed from further analysis. This left ten PD patients and nine controls. Two PD subjects with the longest disease duration (7, 8) had atypical curves (Fig. 2D and 2E) but were retained in the analysis. Basal ganglia region/cerebellum counts/voxel ratios obtained at 180 min were used for subsequent analysis with one exception: one of the subjects (8) (Fig. 2E) was scanned only out to 120 min and the 120 min data for this patient were entered into our calculations in lieu of 180 min data. At 120 min, the basal ganglia/cerebellum ratio was no longer increasing in this subject.

Variability in cerebellar counts/voxel at 180 min was partly, but not entirely, accounted for by variation in dose of radioligand administered (r = 0.718, F = 24.445, p < 0.0005) (Fig. 3). One patient (Patient 3) was rejected because of inadequate counts and an associated artifactual washout curve received 6.28 mCi of IBZM, whereas among patients who were retained in the study because of apparently adequate cerebellar counts, as little as 3.82 mCi of IBZM was administered.
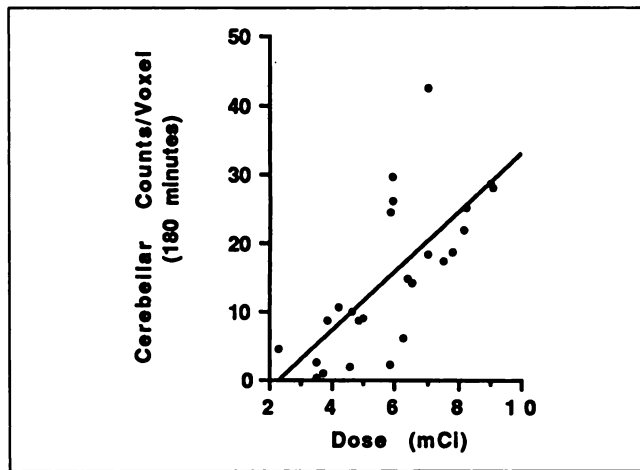
Regional D2 Receptor Density in Relation to Clinical Factors

There were no significant differences between PD patients and control patients in any basal ganglia region/

FIGURE 2. Representative total basal ganglia/cerebellum counts/voxel ratios as a function of time in various subjects. (A) Patient 23. A similarly shaped curve was observed for all subjects retained in the study except Patients 7 and 8. (B) Patient 15. This curve is representative of excluded subjects in whom basal ganglia/cerebellum ratios were artifactually inflated at 180 min because of very low cerebellar counts. (C) Patient 1. This curve is representative of excluded subjects in whom basal ganglia/cerebellum ratios appeared to be artifactually high at 120 min or low at 180 min, apparently also because of low cerebellar counts, although the exact mechanism is unclear. (D) Patient 7. (E) Patient 8. Patients 7 and 8 had distinctive curves, for poorly understood reasons, and were the two patients with disease of the longest duration (16 and 21 yr, respectively).

cerebellum counts/voxel ratio. There was a trend among PD patients toward an inverse correlation between ratios in all regions and levodopa dosage (Table 2) that achieved significance in Cd_V (F = 6.244, p = 0.037) (Fig. 4). Ratios in those on minimal doses of levodopa were similar to ratios in controls. There was a trend toward an inverse correlation between ratios in all regions and disease duration (Table 3) that achieved significance in Put_A (F = 13.144, p = 0.007) (Fig. 5). Ratios in patients with the shortest disease duration were similar to those in controls. The small number of patients precluded a multivariate analysis incorporating both duration of disease and levodopa dosage; however, the correlation between levodopa dosage and disease duration was not significant (r = 0.529, F = 3.116, p = 0.116).

FIGURE 3. Cerebellar counts/voxel at 180 min postinjection as a function of dose of radioligand injected.

Basal ganglia/cerebellum counts/voxel ratios were significantly lower in Put_A among patients with dyskinesias (Table 4 and Fig. 6) (t = 3.068, p = 0.042). Ratios in patients without dyskinesias were similar to those in controls. Because the ratio in Put_A was inversely correlated with duration of disease, and because of the apparent clinical association between dyskinesias and levodopa dosage, we examined the relationships between dyskinesias and both disease duration and levodopa dosage. Neither was statistically significant.

A number of further analyses were performed but failed to show significant effects. There was no relationship between regional ratios and age among controls. Among PD patients, there was no significant relationship between regional ratios and age, sex, presence or absence of deprenyl, or UPDR motor score. We tested the possibility that the most recently administered dose of levodopa might have influenced regional ratios by displacing IBZM (18); despite the fact that time elapsed from last dose ranged from 0.5 to 7.5 hr, no significant relationship was found.
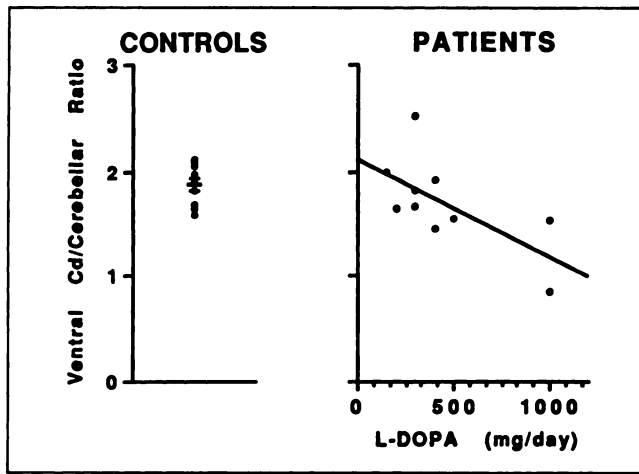
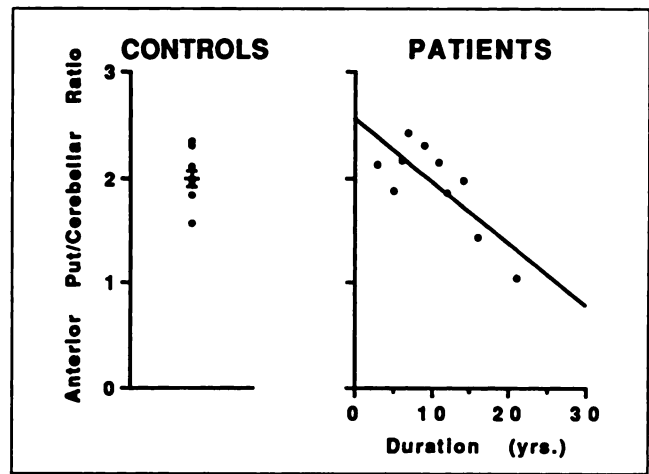## DISCUSSION

Data Acquisition

In this study it proved feasible to measure the D2 receptor density with IBZM and SPECT in the same way that it has been measured with ^{11}C-raclopride and PET (8); that is to compute the ratio between basal ganglia activity (specific + nonspecific binding) and cerebellar activity (non-

TABLE 2
Regression Analysis of Regional Basal Ganglia-to-Cerebellum Ratios and Levodopa Dosage

Region	r	F	p
Cd_V	0.662	6.244	0.037
Cd_D	0.552	3.51	0.098
Put_A	0.403	1.552	0.248
Put_P	0.164	0.222	0.650

FIGURE 4. Ventral caudate/cerebellum counts/voxel ratios in controls (bars: mean ± s.e.) and in PD patients as a function of levodopa dosage.

FIGURE 5. Anterior putamen/cerebellum counts/voxel ratios in controls (bars: mean ± s.e.) and in PD patients as a function of duration of disease.

specific binding) at a time when this ratio has stabilized at an asymptotically approached maximum, the transient equilibrium. With IBZM SPECT this occurs at about 180 min postinjection. Verhoeff et al. (19) found a similar plateau for IBZM SPECT at 150–195 min. When measurements are taken at 120 min postinjection, they fall at the cusp of the basal ganglia/cerebellum ratio curve and are likely to be considerably more susceptible to inaccuracy related to individual variation in time from injection to scan initiation. Because ratios obtained during transient equilibrium are a constant linear function of ratios obtained at true equilibrium (the point of maximum specific uptake) (10), they still provide an acceptable index of B_{max}. Nevertheless, serial scans may be useful for two reasons. First, a temporal plot of ratios enables the identification of ratio curves that are likely to be artifactual in the main because of inadequate radioligand dose. A modest disadvantage of this method was that a dose of over 6 mCi was necessary to assure adequate cerebellar counts at 180 min and a normal ratio curve. This disadvantage and the long period between injection and scan can potentially be addressed by following the initial bolus of radioligand with a constant infusion (10). Second, temporal plots of ratios serve to identify unusual ratio curves, such as those we found in two patients (Fig. 2D and 2E) who were distinguished by the fact that they had the longest disease durations in the study.

Seven subjects were eliminated from this study because

their ratio curves were difficult to interpret. Since they received among the lowest doses of radioligand and they achieved the lowest levels of nonspecific binding (cerebellar counts), we concluded that the ratio curves reflected some kind of artifact. It is clear that in subjects with ratio curves typified by Figure 2B, the relative rate of decline in nonspecific binding (cerebellar counts) began to exceed the relative rate of decline in specific binding, causing the ratios to increase rapidly as cerebellar counts approached zero. The reasons for the artifact exemplified in Figure 2C are uncertain. We retained the subjects with ratio washout curves in Figure 2D and 2E because, even though the curves were aberrant, there was no reason to believe that they reflected experimental artifact.

Many other studies have used basal ganglia/frontal cortex ratios in lieu of basal ganglia/cerebellum ratios. Even though essentially all binding in frontal cortex and cerebellum is nonspecific (within the sensitivity of the method), basal ganglia/frontal ratios of between 1 and 1.18 times basal ganglia/cerebellum ratios have been reported (19,20).

Antiparkinsonian medications were continued without interruption in all our patients. Antonini et al. (18) recently found that several hours of continuous levodopa infusion (60–80 mg/hr, following benserazide) reduced ^{11}C-raclopride binding in the putamen by 20%–27% but not in the

TABLE 3
Regression Analysis of Regional Basal Ganglia-to-Cerebellum Ratios and Disease Duration

Region	r	F	p
Cd$_V$	0.477	2.359	0.163
Cd$_D$	0.314	0.875	0.377
Put$_A$	0.788	13.144	0.007
Put$_P$	0.504	2.719	0.138

TABLE 4
Regional Analysis of Dyskinesias Among Parkinsonian Patients

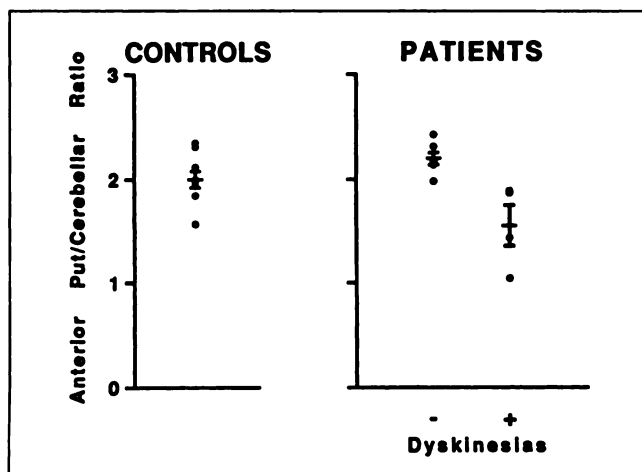| Region | No dyskinesias | | Dyskinesias | | | |
	Mean	s.d.	Mean	s.d.	t	p
Cd$_V$	1.87	0.36	1.44	0.41	1.823	0.118
Cd$_D$	1.95	0.67	1.33	0.25	2.069	0.079
Put$_A$	2.19	0.16	1.55	0.39	3.068	0.042
Put$_P$	1.87	0.24	1.57	0.41	1.354	0.242

FIGURE 6. Anterior putamen/cerebellum counts/voxel ratios in controls and in PD patients without and with dyskinesias (bars: mean ± s.e.).

caudate. Because the affinity of ^{11}C-raclopride and IBZM for D2 receptors is approximately three orders of magnitude greater than that of dopamine (9), the uptake of these ligands is relatively insensitive to modest fluctuations in dopamine. However, it has been shown that in dopamine depleted rats (21), levodopa infusion (100 mg/kg after decarboxylase inhibitor) increases striatal extracellular dopamine 30-fold, compared with less than 2-fold in normal striatum. This difference has been attributed to reduced buffering capacity in denervated striatum as a result of loss of dopamine terminals. Thus, it is possible that our measure of washout ratios were artifactually low as a result of displacement of IBZM by dopamine. We cannot entirely rule out this possibility but we believe it is unlikely for two reasons: (a) there was no significant relationship between time elapsed from last dose of medication, which ranged from 0.5 to 7.5 hr, and regional basal ganglia/cerebellum ratios, and (b) if exogenous dopamine displaced IBZM the effect would have been maximal in the putamen, where endogenous dopamine depletion is most severe. However, we found no relationship between levodopa dosage and the basal ganglia/cerebellum ratios in the putamen—the correlation we found was in the minimally depleted Cd$_V$, consistent with long-term receptor downregulation.

Our method of ROI placement, definition and activity computation is probably as accurate as any that has been used, but it still suffers from significant problems. ROI positioning errors are likely to be less than 2 mm along the x and y axes, but may be as much as 4 mm along the z axis because z-axis placement is most susceptible to errors of rotation about the ear fiducials. With axial scans we were not able to refine the z-axis fiducial-based registration in the way we could the x- and y-axis fiducial based registration, and MRI slices used for ROI placement and definition bore a somewhat variable relationship to the rostro-caudal extent of the basal ganglia. The latter problem could be addressed with thinner MRI slices. Image registration, par-

ticularly with scans in which the brain surface is not well defined (as with dopamine receptor imaging), continues to be a significant problem for functional imaging.

The ROIs we defined were quite small, particularly in the caudate. Because of the limited resolution of SPECT, and because SPECT resolution tends to be poorest at the center of the brain (to which the FWHM rating of 9.3 mm applies), small ROIs lead to underestimation of actual activity within a given structure as a result of volume averaging. This problem is the most serious in the head of the caudate, both because the smallest ROIs were obtained here and caudate measurements involve volume averaging with the cerebrospinal fluid of the frontal horns, as opposed to adjacent white matter as in the putamen. This problem could be addressed only with higher resolution imaging. On the other hand, small, precisely positioned ROIs may more accurately measure actual receptor density and be more sensitive to differences between patient groups. The regional basal ganglia/cerebellum counts/voxel ratios we measured were lower than those measured in in vitro studies of monkey brain (e.g. basal ganglia/cerebellum ratio of 4.93 at 120 min postinjection (22), but were considerably higher than those measured in other functional imaging studies in which ROI placement was probably not as accurate, and ROIs were larger and incorporated more volume averaging with adjacent tissues (20, 23–26).

Statistical Analysis

The relationships between measures of regional basal ganglia D2 receptor density and clinical variables reported in this study need to be viewed with considerable caution. First, multiple measurements were made. Bonferroni correction would have been far too conservative, both because the analysis was in part hypothesis-driven, and because several of the measures were at least partly related. We have chosen instead simply to provide the calculated probabilities and allow the reader to judge them with this caveat in mind. Second, and potentially more serious, the results of this study may be defined by the peculiar attributes of our particular patients, and may not be generally applicable to the PD population at large. This limitation can ultimately only be dealt with through the study of larger numbers of patients.

Comparison with Other Research

This study showed no significant difference between treated PD patients and controls in D2 receptor density in any region of the basal ganglia. A number of postmortem studies have similarly failed to find a difference (3–5). Most of the patients in these studies had been treated at some time with dopaminergic medications but in many these medications were discontinued at some time before death. Time between death and autopsy varied and this may have been a factor contributing to the large individual variability in these studies (27) [see also Bokobza et al. (28) and Cash et al. (3)]. Patient heterogeneity may also have been a significant contributing factor (29). Several functional im-

aging studies with PET (30,31) and SPECT (24,32,33) have failed to find a difference in receptor density between actively treated PD patients and controls.

Even though we found no evidence of an overall difference in receptor density between PD patients and controls, we did find evidence of an inverse relationship between levodopa dosage and receptor density, statistically significant in Cd_V. Further evidence that dopaminergic treatment may suppress receptor density has been found in biopsy (29), postmortem (34), and SPECT (20,25,35,36) studies demonstrating reduced receptor density in treated PD patients compared with controls. It has been found in postmortem (37,38) and PET (8,39-43) studies showing increased receptor density in untreated PD patients compared with controls. It has also been found in PET (39,43,44) and SPECT studies showing increased receptor density in the basal ganglia contralateral to the side of maximum symptoms (24-26,45). Unfortunately, there are also many functional imaging studies that have failed to find differences in receptor density between untreated PD patients and controls (20,24-26,33,35). Two studies have found increased receptor density in treated PD patients compared to untreated patients (46) or controls (28), findings that are difficult to reconcile with the results of other investigations.

The differential relationship we found between levodopa dosage and Cd_V receptor density is logical. Because PD patients are treated to achieve normal dopamine levels in the putamen where dopamine depletion is most severe and is responsible for most symptoms, excessive dopamine levels are likely to be attained in Cd_V, where dopamine depletion tends to be modest and the addition of exogenous dopamine is likely to result in supranormal levels. Excess dopamine levels in Cd_V would logically lead to receptor down-regulation. Our patients were generally receiving low doses of dopaminergic agents (levodopa and deprenyl only, except in one case). It may be that higher doses would have lead to excessive dopamine levels throughout the basal ganglia, generalized down-regulation of receptors, and loss of the differential effect in Cd_V.

We found a significant inverse correlation between D2-receptor density and disease duration in Put_A, and we found that Put_A receptor density was significantly lower in patients with dyskinesias. The relationship of receptor density to disease duration is a novel one, not demonstrated so far in other studies (3,5,8,20,47), and we cannot entirely rule out the possibility that the effect can be explained by a trend toward higher dosage of dopaminergic agents in late disease (not statistically significant in this study). We did not have sufficient subjects to perform a multivariate analysis. Hierholzer et al. (20), in a study of 25 patients, did find a receptor density decline with advancing disease but this effect disappeared when controlled for levodopa dose. Two functional imaging studies (8,33,36) have found a significant reduction in basal ganglia D2-receptor density in patients with dyskinesias, whereas Pierot et al. (5) failed to find a difference in a postmortem study.

The differential relationship between D2-receptor density and duration of disease in Put_A and the association between low receptor density and dykinesias found in the putamen in the present investigation and in the basal ganglia in general in other studies (8,33,36) raise many questions. Neither finding is likely to reflect receptor down-regulation by high dopamine levels because our patients remained symptomatic (see UPDR motor scale in Table 1) and thus almost certainly had inadequate dopamine levels in the putamen. By conventional reasoning, there should have been upregulation of putamenal dopamine receptors in these patients. However, a detailed neurophysiologic explanation for dyskinesias (typically seen with long-duration disease) has not been established or supported with animal or human studies, and therefore, our results raise some alternative possibilities. First, if alterations in receptor density do occur with time and are related to dopamine deficiency, then they are most likely to occur in those regions, such as the putamen, in which dopamine depletion is most severe, and in which moment-to-moment dopamine levels are most closely linked to the pattern of administration of dopaminergic medication and are most deviant from the natural temporal pattern (48). However, dopamine is severely depleted in both Put_A and Put_P, so it is not clear why the strongest relationship between receptor density and disease duration should be found in Put_A. Second, as animal studies have shown, dopamine depletion should lead to an increase in receptor density (49).

Declines in receptor density raise the question of a second pathologic process going on in the striatum itself. Guttman et al. (47) raised the possibility that D2 receptor loss might be due to transynaptic degeneration of striatal neurons. Some studies have demonstrated complex changes in a variety of neuropeptide neurotransmitters within the striatum in PD (Bravi et al. (48)). McNeill et al. (50) have demonstrated dendritic pathology involving medium spiny type I neurons in the basal ganglia of PD patients that may be caused by transynaptic degeneration, or may simply be part of the spectrum of pathology in PD. Third, the reason for the particular association between Put_A D2 receptor loss and dyskinesias is uncertain but may reflect the particular motor systems supported by Put_A as compared to Put_P (2,51). The putamen is organized somatotopically along the dorso-ventral axis, suggesting that there may be functional heterogeneity along the anterior-posterior axis (52). Finally, although it is generally assumed that supersensitivity of D2 receptors underlies the emergence of levodopa-induced involuntary movements (53), our study and others (8,33) suggest otherwise. In fact, the precise mechanism by which alterations in receptor density might lead to dyskinesias still remains unknown.

ACKNOWLEDGMENTS

REFERENCES

1. Agid Y, Bonnet A-M, Ruberg M, Javoy-Agid F. Pathophysiology of L-dopa-induced abnormal involuntary movements. In: Casey DE, Chase TN, Christensen AV, Gerlach J, ed. Dyskinesia. Research and treatment. Berlin: Springer-Verlag; 1985:145–159.
2. Crossman AR. A hypothesis on the pathophysiological mechanisms that underlie levodopa- or dopamine agonist-induced dyskinesia in Parkinson's disease: implications for future strategies in treatment. Mov Disord 1990;5: 100–108.
3. Cash R, Raisman R, Ploska A, Agid Y. Dopamine D-1 receptor and cyclic AMP-dependent phosphorylation in Parkinson's disease. J Neurochem 1987;49:1075–1083.
4. Cortés R, Camps M, Gueye B, Probst A, Palacios J. Dopamine receptors in human brain: autoradiographic distribution of D1 and D2 sites in Parkinson syndrome of different etiology. Brain Res 1989;483:30–38.
5. Pierot L, Desnos C, Blin J, et al. D1 and D2-type dopamine receptors in patients with Parkinson's disease and progressive supranuclear palsy. J Neurosci 1988;86:291–306.
6. Kung HF, Alavi A, Chang W, et al. In vivo SPECT imaging of CNS D2 dopamine receptors: initial studies with iodine-123-IBZM in humans. J Nucl Med 1990;31:573–579.
7. Antonini A, Leenders KL, Reist H, Thomann R, Beer H-F, Locher J. Effect of age on D2 dopamine receptors in normal human brain measured by positron emission tomography and ¹¹C-raclopride. Arch Neurol 1993;50: 474–480.
8. Brooks DJ, Ibanez V, Sawle GV, et al. Striatal D2 receptor status in patients with Parkinson's disease, striatonigral degeneration, and progressive supranuclear palsy, measured with ¹¹C-raclopride and positron emission tomography. Ann Neurol 1992;31:184–192.
9. Farde L, Hall H, Ehrin E, Sedvall G. Quantitative analysis of D2 dopamine receptor binding in the living human brain by PET. Science 1986;231:258–261.
10. Carson RE, Channing MA, Blasberg RG, et al. Comparison of bolus and infusion methods for receptor quantitation: application to [¹⁸F]cyclofoxy and positron emission tomography. J Cereb Blood Flow Metab 1993;13:24–42.
11. Kish SJ, Shannak K, Hornykiewicz O. Uneven pattern of dopamine loss in the striatum of patients with idiopathic Parkinson's disease. Pathophysiologic and clinical implications. N Engl J Med 1988;318:876–880.
12. Stern MD. Rating the Parkinsonian patient. In: Stern MB, Hurtig HI, ed. The comprehensive management of Parkinson's disease. New York: PMA Publishing Corp., 1988:3–50.
13. Hoen MM, Yahr MD. Parkinsonism: onset, progression and mortality. Neurology 1967;17:427–442.
14. Folstein MF, Folstein SE, McHugh PR. Mini-mental state. A practical method for grading the cognitive state of patients for the clinician. J Psychol Res 1975;12:189–198.
15. Kung M-P, Kung HF. Peracetic acid as a superior oxidant for the preparation of [¹²³I]IBZM: a potential dopamine D-2 receptor imaging agent. J Lab Cmpd Radiopharm 1989;27:691–700.
16. Shukla SS, Honeyman JC, Crosson B, Williams CM, Nadeau SE. Method for registering brain SPECT and MR images. J Comput Assist Tomogr 1992;16:966–970.
17. Damasio H, Damasio AR. Lesion analysis in neuropsychology. New York: Oxford University Press; 1989.
18. Antonini A, Schwarz J, Oertel WH, Beer HF, Madeja UD, Leenders KL. [¹¹C]raclopride and positron emission tomography in previously untreated patients with Parkinson's disease: influence of L-dopa and lisuride therapy on striatal dopamine D2 receptors. Neurology 1994;44:1325–1329.
19. Verhoeff NPLG, Brücke T, Podreka I, Bobeldijk M, Angelberger P, Van Royen EA. Dynamic SPECT in two healthy volunteers to determine the optimal time for in vivo D2 dopamine receptor imaging with ¹²³I-IBZM using the rotating gamma camera. Nucl Med Commun 1991;12:687–697.
20. Hierholzer VJ, Cordes M, Schelosky L, et al. Bestimmung der zerebralen Dopamin-(D2)-Rezeptoren-Dichte mit Hilfe der ¹²³Jod-IBZM-SPECT bei Patienten mit Morbus Parkinson. Fortschr Röntgenstr 1992;157:390–398.
21. Abercrombie ED, Jacobs BL. Dopaminergic modulation of sensory responses of striatal neurons: single unit studies. Brain Res 1985;358:27–33.
22. Kung HF, Pan S, Kung M-P, et al. In vitro and in vivo evaluation of [¹²³I]IBZM: a potential CNS D-2 dopamine receptor imaging agent. J Nucl Med 1989;30:88–92.
23. Tatsch K, Schwarz J, Oertel WH, Kirsch C-M. SPECT imaging of dopamine D2 receptors with I-123 IBZM in Parkinsonian syndromes [Abstract]. J Nucl Med 1991;32:1014–1015.
24. Tatsch K, Schwarz J, Oertel WH, Kirsch C-M. Idiopathic Parkinson syn-

drome: I-123 IBZM SPECT findings in drug naïve and treated patients [Abstract]. Eur J Nucl Med 1992;19:609.
25. Hertel A, Baas H, Maul FD, et al. D2 dopamine receptor scintigraphy with I-123 IBZM in hemiparkinson and denovo Parkinson disease. Eur J Nucl Med 1992;19:610.
26. Schwarz J, Tatsch K, Arnold G, et al. Iodine-123 I-iodobenzamide-SPECT predicts dopaminergic responsiveness in patients with de novo parkinsonism. Neurology 1992;42:556–561.
27. Rinne UK, Lönnberg P, Koskinen V. Dopamine receptors in Parkinsonian brain. J Neural Transm 1981;51:97–106.
28. Bokobza B, Ruberg M, Scatton B, Javoy-Agid F, Agid Y. [³H]spiperone binding, dopamine and HVA concentrations in Parkinson's disease and supranuclear palsy. Eur J Pharmacol 1984;99:167–175.
29. Ahlskog JE, Richelson E, Nelson A, et al. Reduced D2 dopamine and muscarinic cholinergic receptor densities in caudate specimens from fluctuating Parkinsonian patients. Ann Neurol 1991;30:185–191.
30. Hägglund J, Aquilonius S-M, Eckernäs S-Å, et al. Dopamine receptor properties in Parkinson's disease and Huntington's chorea evaluated by positron emission tomography using ¹¹C-N-methyl-spiperone. Acta Neurol Scand 1987;75:87–94.
31. Wienhard K, Coenen HH, Pawlik G, et al. PET studies of dopamine receptor distribution using [¹⁸F]fluoroethylspiperone: findings in disorders related to dopaminergic system. J Neural Transm 1990;81:195–213.
32. Tatsch K, Schwarz J, Oertel WH, Kirsch C-M. SPECT imaging of dopamine D2 receptors with ¹²³I-IBZM: initial experience in controls and patients with Parkinson's syndrome and Wilson's disease. Nucl Med Commun 1991;12:699–707.
33. Pizzolato G, Rossato A, Briani C, et al. Alterations of striatal D2 receptors contribute to deteriorated response to L-dopa in Parkinson's disease (PD): a ¹²³IBZM SPECT study [Abstract]. Neurology 1993;43:270.
34. Reisine TD, Fields JZ, Yamamura HI, et al. Neurotransmitter receptor alterations in Parkinson's disease. Life Sci 1977;21:335–344.
35. Brücke T, Podreka I, Angelberger P, et al. Dopamine D2 receptor imaging with SPECT: studies in different neuropsychiatric disorders. J Cereb Blood Flow Metab 1991;11:220–228.
36. Pizzolato G, Chierichetti F, Rossato A, et al. Dopamine receptor SPECT imaging in Parkinson's disease: a [¹²³I]IBZM and [⁹⁹ᵐTc]-HM-PAO study. Eur Neurol 1993;33:143–148.
37. Guttman M, Seeman P. L-DOPA reverses the elevated density of D2 dopamine receptors in Parkinson's diseased striatum. J Neural Transm 1985; 64:93–103.
38. Lee T, Seeman P, Rajput A, Farley IJ, Hornykiewicz O. Receptor basis for dopaminergic supersensitivity in Parkinson's disease. Nature 1978;273:59–61.
39. Brooks DJ. PET studies on the early and differential diagnosis of Parkinson's disease. Neurology 1993;43:S6–S16.
40. Snow B, Buckley K, Bailey D, et al. Dopamine D2 receptor density is inversely correlated with dopaminergic innervation in untreated Parkinson's disease [Abstract]. Neurology 1993;43:269.
41. Rinne UK, Laihinen A, Rinne JO, Någren K, Bergman J, Ruotsalainen U. Positron emission tomography demonstrates dopamine D2 receptor supersensitivity in the striatum of patients with early Parkinson's disease. Mov Disord 1990;5:55–59.
42. Sawle GV, Brooks DJ, Ibanez V, Frackowiak RSJ. Striatal D2 receptor density is inversely proportional to DOPA uptake in untreated hemi-Parkinson's disease: a positron emission tomographic study [Abstract]. J Neurol Neurosurg Psychiatry 1990;53:177.
43. Sawle GV, Playford ED, Brooks DJ, Quinn N, Frackowiak RSJ. Asymmetrical presynaptic and postsynaptic changes in the striatal dopamine projection in dopa naïve parkinsonism. Brain 1993;116:853–867.
44. Rinne JO, Laihinen A, Någren K, et al. PET demonstrates different behavior of striatal dopamine D-1 and D-2 receptors in early Parkinson's disease. J Neurosci Res 1990;27:494–499.
45. Laulumaa V, Kuikka JT, Soininen H, Bergström K, Länsimies E, Riekkinen P. Imaging of D2 dopamine receptors of patients with Parkinson's disease using single photon emission computed tomography and iodobenzamide I-123. Arch Neurol 1993;50:509–512.
46. Rutgers AWG, Lakke JPWF, Raans AMJ, Vaalburg W, Kork J. Tracing of dopamine receptors in hemiparkinsonism with positron emission tomography. J Neurosci 1987;80:237–248.
47. Guttman M, Seeman P, Reynolds GP, Riederer P, Jellinger K, Tourtellotte WW. Dopamine D2 receptor density remains constant in treated Parkinson's disease. Ann Neurol 1986;19:487–492.
48. Bravi D, Mouradian MM, Roberts JW, Davis TL, Sohn YH, Chase TN.

± Wearing-off fluctuations in Parkinson's disease: contribution of postsynaptic mechanisms. *Ann Neurol* 1994;36:27-31.

49. Rinne UK. Brain neurotransmitter receptors in Parkinson's disease. In: Marsden CD, Fahn S, ed. *Movement disorders*. London: Butterworth Scientific, 1982:59-74.

50. McNeill TH, Brown SA, Rafals JA, Shoulson I. Atrophy of medium spiny I striatal dendrites in advanced Parkinson's disease. *Brain Res* 1988;455: 148-152.

51. Hoover JE, Strick PL. Multiple output channels in the basal ganglia. *Science* 1993;259:819-821.

52. Beckstead RM, Wooten GF, Trugman JM. Distribution of D1 and D2 dopamine receptors in the basal ganglia of the cat determined by quantitative autoradiography. *J Comp Neurol* 1988;268:131-145.

53. Agid Y, Cervera P, Hirsch E, et al. Biochemistry of Parkinson's disease 28 years later: a critical review. *Mov Dis* 1989;4(suppl 1):126-144.

FIRST IMPRESSIONS
Multifocal Avascular Necrosis

FIGURE 1.

FIGURE 2.

PURPOSE

A 37-yr-old female was referred for bone scanning of bilateral knee pain. The bone scan (Fig. 1) showed multiple areas of increased activity in both knees, suggesting degenerative arthritis. The x-rays were negative. MRI, however, showed multiple foci of avascular necrosis (Fig. 2) that correspond to hot areas on the bone scan.

TRACER

Technetium-99m-MDP

ROUTE OF ADMINISTRATION

Intravenous

TIME AFTER INJECTION

2.50 hours

INSTRUMENTATION

Whole-body camera

CONTRIBUTOR

M. Moinuddin, Baptist Memorial Hospital, Memphis, Tennessee